Convergence
A Journal for Young Researchers

ORIGINAL REVIEW

Received: 8-28-25; Accepted: 11-5-25;
Managing Editor: Jonas Katona;
Action Editor: Jonas Katona

A Fifth Fundamental Force? A Comparative Review Between ΛCDM and Quintessence

Thatcher Lai

Rugby School, Rugby, Warwickshire, England

Abstract

The nature of dark energy remains one of the most important unsolved problems in cosmology today. The Lambda Cold Dark Matter (ΛCDM) model is currently the most widely accepted model of the Big Bang theory, describing dark energy using a cosmological constant Λ. However, discrepancies arise when attempting to determine its actual value, and predictions from theories differ from observations; issues like these suggest the need for alternative dark energy models. This review paper primarily focuses on whether ΛCDM is still the most plausible model for dark energy and if quintessence is a suitable alternative. This paper first gives an overview of observational evidence for dark energy and a review of ΛCDM. Then, the current issues with ΛCDM are discussed. Next, a modified dark energy model, quintessence, is explored. Finally, this paper analyzes and compares their compatibilities with observational evidence. It is concluded that quintessence is generally preferred over ΛCDM, but observational data also suggest a deviation from quintessence at higher redshifts, thus slightly favoring quintom models (which combine quintessence and phantom behavior), w_0w_aCDM, and $w_0w_aw_b$CDM over quintessence and ΛCDM. Current observational data are also limited in terms of their ability to meaningfully constrain dark energy parameters.

Keywords: dark energy, quintessence, ΛCDM (Lambda Cold Dark Matter model), cosmological constant problem, Hubble tension, equation of state (EoS)

1. Introduction

We can only see about 4% of the universe. That is, only 4% of the universe is made up of atoms (or “ordinary matter”), and the rest is dark energy (73%) and dark matter (23%) (Coble et al., 2013). Dark matter is a hypothetical form of matter that does not interact with light, but its existence has been inferred from gravitational effects observed at various scales in the universe (Mayet et al., 2016). Many observations suggest that our universe undergoes accelerated expansion (Riess et al., 1998), leading to the proposal of dark energy — a hypothetical form of energy with negative pressure that causes this

expansion. Decades of research and observations have been conducted, but the natures of dark matter and dark energy remain a mystery today.

Einstein (1915) developed the Einstein field equations (EFEs), which relate matter and energy in the universe to the geometry of spacetime. The EFEs were a turning point in physics, showing how Newtonian physics was not enough to describe the dynamics of astronomical bodies fully. Einstein (1917) then proposed adding a cosmological constant Λ to the EFEs to obtain a solution for a static and homogeneous universe (which was believed to be the case at the time); this served to counteract the effect of gravitational attraction within the universe. However, Hubble (1929) discovered that the universe was expanding, leading Einstein to remove Λ from the EFEs (Li et al., 2011). This discovery had profound implications, as it meant that there was an unknown component of the universe propelling its expansion; hence, Λ was reintroduced by Zel'Dovich (1968). Following this discovery, Sandage (1962) introduced the deceleration parameter q_0, a quantity describing the decelerating rate of expansion of the universe, as it was believed that the universe's expansion was slowing. In the following decades, many cosmologists focused on measuring the values of q_0 and Hubble's parameter H, a quantity that describes the ratio between the relative recession velocity of distant celestial bodies and their distances (Hubble, 1929). In 1998 and 1999, observations from various supernovae supported the idea that the universe's expansion rate was accelerating (Peebles et al., 2003; Perlmutter et al., 1999; Riess et al., 1998). Since then, many alternative dark energy and gravity models have been proposed (Abbott et al., 2016; Caldwell et al., 1998; Gu et al., 2009; Liddle et al., 2006; Tutusaus et al., 2024), and various observations have been made to test the validity of different models (Abbott et al., 2016; Gu et al., 2009; Liddle et al., 2006; Tutusaus et al., 2024).

This paper first reviews the observational evidence for dark energy, including observed redshift from supernovae and BAOs. Then, it explores the core ideas and issues in ΛCDM that imply beyond-ΛCDM physics. The subsequent sections examine the physics of quintessence, a modified dark energy model that has gained prevalence over the decades due to its relatively simple formulation and better fit to the data than ΛCDM (Steinhardt, 2003), and evaluate whether ΛCDM is still the most conceivable model for dark energy. This paper looks at the predicted evolution of the equations of state (EoS) for freezing and thawing quintessence, which, along with the Friedman equations (FEs), determine the evolution of the universe. This paper also aims to provide a comparative review of the plausibility of quintessence relative to ΛCDM as a supplement to the existing literature by comparing predictions to observational data and discussing its strengths and limitations. This paper shows that ΛCDM does not remain the most plausible dark energy model and that a dynamical model better fits observational data.

SI units are used in this paper. Einstein's summation notation (ESN) is assumed throughout. For a review of ESN, see the Appendix.

2. Observational Evidence for Dark Energy

This section provides a brief overview of the two primary pieces of observational evidence supporting the existence of dark energy: observations from Type Ia supernovae and baryon acoustic oscillations.

2.1. Type Ia Supernovae

SNe Ia are a type of standard candle (astronomical objects with known luminosities). These supernovae occur in binary star

systems when a white dwarf exceeds 1.44 times the mass of the Sun (called the Chandrasekhar mass) and reignites (Chandrasekhar, 1931; Janka et al., 2007). This happens when electron degeneracy pressure can no longer withstand gravity, and the star collapses, exploding into a supernova. Because white dwarfs have a fixed Chandrasekhar mass, their peak luminosity is predictable, and by measuring the apparent magnitude, one can deduce their distance from Earth.

Cosmological redshift occurs when a source in the universe that emits a specific wavelength of light becomes more distant from an observer due to the expansion of the universe itself, resulting in the observer seeing a longer wavelength of light. The cosmological redshift z of an object emitting light with wavelength λ_0 and observed wavelength λ is calculated using the following equation:

$$z = \frac{\lambda - \lambda_0}{\lambda_0}. \tag{2.1}$$

Another related quantity is the scale factor $a(t)$, which describes the size of the universe relative to its current size. t denotes cosmic time, which is the time elapsed since the Big Bang in a reference frame where the CMB does not appear to have any redshift and the average velocity of matter in the universe is zero. Cosmic time can be thought of as an "absolute" time, taking the universe's expansion into account (Bamonti & Thébault, 2025). $a(t_0) = 1$ denotes the scale factor at the current age of the universe t_0. The scale factor a as a function of z is given by:

$$a(z) = \frac{1}{1+z}. \tag{2.2}$$

Riess et al. (1998) observed SNe Ia with redshifts between 0.16 and 0.62 and found that the distances were 10–15% further and dimmer than expected. As a result, a positive Λ with 3.0–4.0σ confidence and a negative deceleration parameter with 2.8–3.9σ confidence were determined. Perlmutter et al. (1999) measured 42 SNe Ia with redshifts between 0.18 and 0.83 and determined with 99% confidence that $\Lambda > 0$. These results imply that the universe is likely undergoing accelerated expansion, with many other observations supporting this (Aghanim et al., 2020; Eisenstein et al., 2005). This means that the recessional velocities of galaxies relative to Earth at higher redshifts increase, and that the Hubble constant H_0 changes over time.

2.2. Baryon Acoustic Oscillations

Analogous to how SNe Ia are used as standard candles, BAOs are used as standard rulers, which are objects with a known physical size. In the early stages of the universe, photons and matter existed as plasma (where particles are ionized and electrons are unbound to atoms). Where there were higher densities of this plasma, gravity caused it to attract, and pressure caused it to expand, resulting in oscillations with largely fixed wavelengths in the plasma, like sound waves. These oscillations are referred to as BAOs. Afterwards, when the plasma cooled and neutral atoms formed (called the recombination phase), photons were able to travel freely without colliding with electrons frequently, forming the cosmic microwave background (CMB). Over time, the higher-density regions of baryonic matter left behind from the plasma, known as sound horizons, formed stars and galaxies. By measuring the apparent sizes of these sound horizons at different redshifts, one can determine the rate of expansion of the universe (Abbott et al., 2024). Eisenstein et al. (2005) found that the actual size of a sound horizon is around 490 million light-years. These largely fixed separation distances are due to the pressure waves being "frozen" after recombination. Blake et al. (2011) used BAOs to conclude with 99.8% confidence that the

universe is undergoing accelerated expansion.

3. ΛCDM and the Cosmological Constant

This section reviews the core concepts of ΛCDM. The EFEs, FEs, and EoS are discussed first. Then, the Hubble tension and the cosmological constant problem of ΛCDM are examined. The EFEs relate the mass-energy content (right side of Equation 3.1) in the universe to the curvature of spacetime (left side of Equation 3.1). They are given (in component form) by

$$R_{\mu\nu} - \frac{1}{2}Rg_{\mu\nu} + \Lambda g_{\mu\nu} = \frac{8\pi G}{c^2}T_{\mu\nu}, \tag{3.1}$$

where $R_{\mu\nu}$ (the Ricci tensor) and R (the Ricci scalar) describe the local curvature of spacetime, $g_{\mu\nu}$ is the metric tensor (which one can think of as a "bar scale" at each point in a manifold, indicating how a local patch of geometry is stretched or squished and how measurements of length change), Λ is the cosmological constant, G is the gravitational constant, c is the speed of light, and $T_{\mu\nu}$ is the stress-energy tensor (which describes the energy and momentum flux in temporal and spatial dimensions). Friedmann (1922) derived the FEs from the EFEs based on the assumptions that the universe, at large scales, is expanding with a time-varying scale factor $a(t)$ for cosmic time t, has uniform energy density $\rho = T_{00}$ (the zeroth temporal component of $T_{\mu\nu}$), and has uniform pressure $a^2p = a^2(p_x + p_y + p_z) = T_{ii}$ (the sum of the diagonal spatial components of $T_{\mu\nu}$), where both ρ and p account for the radiation, baryonic and dark matter, and dark energy in the universe. That is, the universe is assumed to be a perfect fluid, spatially isotropic, and homogeneous. The coefficient a^2 of the spatial part of the stress-energy tensor signifies the spatial expansion of the universe.

The FEs describe the expansion of the universe in terms of the scale factor and its derivatives, given its mass-energy content and curvature. The first FE is given by

$$H^2 = \left(\frac{\dot{a}}{a}\right)^2 = \frac{8\pi G\rho}{3c^2} - \frac{kc^2}{a^2} + \frac{\Lambda c^2}{3}, \tag{3.2a}$$

where $H = \dot{a}/a$ is the Hubble parameter and k is the curvature parameter of the universe, which can be positively curved (+1), flat (0), or negatively curved (−1). The above equation compares the rate of the universe's expansion to its scale and relates it to the mass-energy content of the universe. The second FE is given by

$$\frac{\ddot{a}}{a} = -\frac{4\pi G}{3c^2}(\rho + 3p) + \frac{\Lambda c^2}{3}, \tag{3.2b}$$

which compares the acceleration of the universe's expansion to its scale. The FEs are important because different dark energy models use them to predict different evolutions of the universe (i.e., different Hubble parameters). The EoS of dark energy is given by the ratio of pressure p to energy density ρ for a perfect fluid: $w = p/\rho$. In ΛCDM, the EoS for dark energy equals −1, meaning its pressure and energy density are constant in time and $p = -\rho$. Other components of the universe, including radiation, ordinary matter, and dark matter, have different values of w, so w itself is not unique to dark energy. The EoS is useful because it determines the dynamics of dark energy and how it drives the expansion of the universe. It is also one of the many important parameters measured by probes (T. M. C. Abbott et al., 2025; Abdul-Karim et al., 2025).

While the EFEs and FEs are well-established equations in that the EFEs give extremely accurate predictions of the behavior of astronomical objects and that the FEs are derived from the EFEs, huge issues exist in experimentally verifying the value of H, and disagreements arise in different physical theories of Λ.

3.1. Hubble Tension

In ΛCDM, dark energy is modeled using a cosmological constant Λ. Astronomers use various methods to determine the present-day value of $H(t)$, called the Hubble constant H_0, with methods including measuring distances using standard candles such as Cepheids (pulsating stars) and SNe Ia, as well as measuring redshifts of galaxies (Riess et al., 1998, 2019). These methods then help determine the scale factor a and solve for H via the FEs.

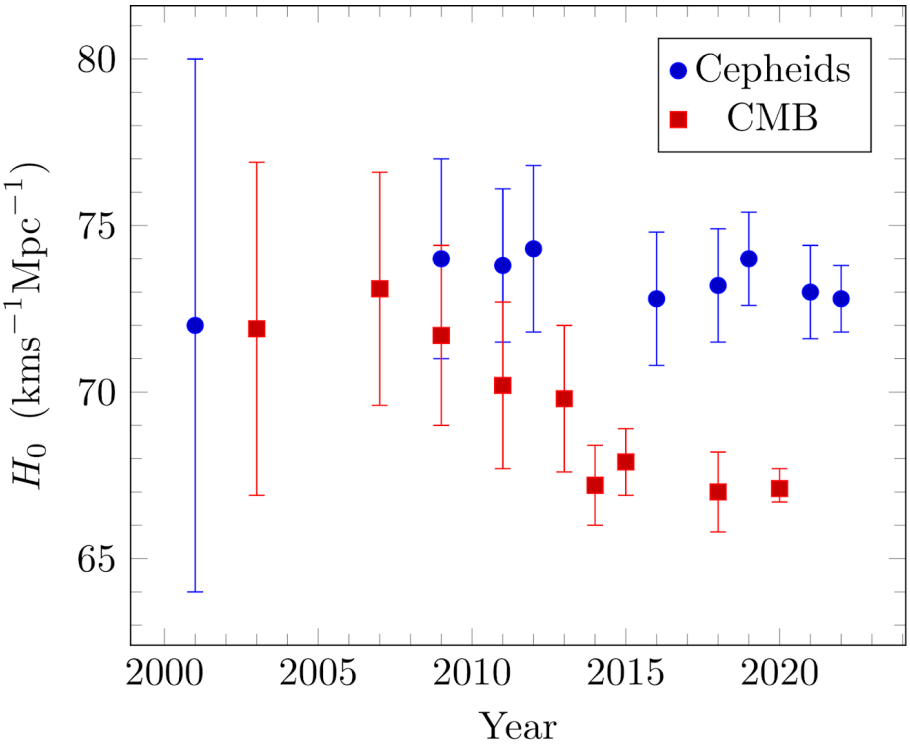

Figure 1. Various measurements of the Hubble constant H_0 from Cepheids (blue) and CMB data (red) from 2001 to 2022. A major discrepancy between the measured value of H_0 exists. Reproduced from (Perivolaropoulos & Skara, 2022).

However, a major disagreement exists between measurements of the value of H_0. The 2018 Planck collaboration determined a value of $H_0 = 67.36 \pm 0.54$ km s^{-1} Mpc^{-1}, whereas the 2024 SH0ES collaboration measured a value of 73.17 ± 0.86 km s^{-1} Mpc^{-1} at a $>5\sigma$ tension with the Planck collaboration (Zhou et al., 2025). The cause of this discrepancy is unknown and is a huge problem for cosmology as it indicates potential systematic errors in our measurements or a fundamental flaw in ΛCDM, requiring new developments in measurement techniques and mathematical models. Different measurements of H_0 from 2001 to 2022 are shown with error bars in Figure 1.

3.2. Cosmological Constant Problem

The cosmological constant problem refers to a discrepancy between the observed and predicted values of the vacuum energy density (vacuum energy per cubic meter) $\rho_\Lambda = \Lambda c^4/8\pi G$ (and hence Λ). Quantum field theory (QFT) comprises special relativity, quantum mechanics, and classical field theory; it is currently one of the most complete and successful physical theories and is used to formulate the Standard Model of particle physics. In QFT, the zero-point energy of a vacuum (also called the vacuum energy) refers to the minimum amount of energy a vacuum can have. Dark energy is a form of vacuum energy where the vacuum energy density is constant, which means that the total amount of dark energy increases as the universe expands. Weinberg (1989) calculated that the predicted value of Λ in QFT (2×10^{109} J m^{-3}) is around 120 orders of magnitude larger than the observed value (2×10^{-11} J m^{-3}) (Yoo & Watanabe, 2012). This discrepancy is a massive problem as it demonstrates the current incompatibility between theory and cosmological observations; this may require significant reformulation of QFT or theories of cosmology, fundamentally changing our understanding of dark energy.

Current measurements suggest that the universe is extremely flat (i.e., the curvature parameter k is essentially zero). The curvature of the universe is affected by its mass-energy content. The critical density ρ_c is defined as the energy density (of all the content of the universe, including matter, radiation, and dark energy) required for $k = 0$, where we define the ratio ρ/ρ_c as the density parameter Ω. The Wilkinson Microwave Anisotropy Probe (WMAP) and the Supernova Legacy Survey (SNLS) measured $\Omega = 1$ with around 1% deviation (Spergel et al., 2007). Observations also suggest that the density parameter for matter is $\Omega_m \approx 0.3$, and that for dark energy is $\Omega_\Lambda \approx 0.7$. The coincidence problem then asks the question of why Ω_m and Ω_Λ are of the same order of magnitude today, despite evolving very differently in the past. Since the universe is measured to be very flat (i.e., $\Omega \approx 1$ and $\rho \approx \rho_c$), this suggests that if ρ_m or ρ_Λ were to slightly deviate away from the critical value, over time, this would result in drastically different evolutions of the universe, including the Big Crunch (where gravity collapses the universe) and the Big Freeze (where the universe grows cold) (Zlatev et al., 1999). Problems such as the Hubble tension, the cosmological constant problem, and the coincidence problem imply the need for new models of dark energy, with one such being quintessence.

4. Quintessence

There are two general types of modified dark energy models. Those that change the left side of the EFEs (Equation 3.1) result in modified gravity models, and those that change the right side result in modified matter models (Tsujikawa, 2013; Yoo & Watanabe, 2012). This paper will focus on quintessence (a term coined by Caldwell et al. (1998)), which is a modified matter model. It is one of the simplest alternatives to Λ involving a change to the stress-energy tensor $T_{\mu\nu}$. Quintessence is postulated as a "fifth fundamental force" that interacts gravitationally with matter and dismisses the requirement of Λ, instead modelling dark energy using a time-dependent and (on large scales) homogeneous scalar field $\varphi(x^\mu)$, with spacetime coordinates x^μ and a potential energy $V(\varphi)$ that gradually decreases to a minimum (Steinhardt, 2003; Yoo & Watanabe, 2012). This contrasts with ΛCDM in that its dark energy EoS remains constant through time. Due to Λ's constancy, ΛCDM is easier to falsify since any significant deviation from $w = -1$ would strongly indicate its implausibility, whereas quintessence is dynamic and can take on multiple evolutions of w, so it is harder to falsify.

One of the weaknesses of quintessence is that it does not solve the Hubble tension nor the cosmological constant problem, but it does partially solve the coincidence problem, which arises due to the energy density of dark energy ρ_Λ and matter ρ_m in the universe decreasing at different rates, hence requiring their initial values to be fine-tuned (Zlatev et al., 1999).

Quintessence addresses this problem by providing a "tracking" behavior of φ where the EoS for quintessence roughly equals the EoS for radiation during the radiation-dominated epoch and that for matter during the matter-dominated epoch of the universe, with the EoS of quintessence only recently becoming dominant. This allows a wide range of initial values for φ to lead to the same evolution of w. However, this means that the potential V must still be fine-tuned. Despite its weakness, physicists still consider quintessence as a possible dark energy candidate because if the equation of state of dark energy turns out to be non-constant, then quintessence and ΛCDM can be observationally distinguished. We can also study the physical motivations behind quintessence and apply some of its principles to other dark energy models. Quintessence may also reconcile problems that arise in particle physics and effective field theory whilst being more physically motivated than ΛCDM (Souza et al., 2025); this is because Λ is a term arbitrarily added to accommodate for the universe's accelerated expansion, whereas the universe's acceleration and the dark energy EoS may vary with cosmic time, which a dynamical scalar field may more accurately describe.

Dark energy possesses an energy density and pressure, and we require that a mathematical description of these quantities remain the same regardless of what coordinates are used. To encapsulate this, one uses the stress-energy tensor $T_{\mu\nu}$, which, for the quintessence field φ, is given by (Copeland et al., 2006; Li et al., 2011)

$$T_{\mu\nu} = \partial_\mu\varphi\partial_\nu\varphi - g_{\mu\nu}\left[\frac{1}{2}\partial^\alpha\partial_\alpha\varphi + V(\varphi)\right], \tag{4.1}$$

where $g_{\mu\nu}$ is the metric tensor, and ∂_μ and ∂^μ denote 4-gradients (which are four-dimensional derivatives in time and space), respectively. The above equation shows how the pressure and energy of the quintessence field depend on its rate of change in spacetime and its potential energy. The stress-energy tensor can be used to determine the EoS of quintessence, which can then predict the universe's expansion history and fate. It is assumed that pressure and energy density are measured in the local rest frame of an observer comoving with the quintessence field; that is, the observer "moves along" with the expansion of the universe such that it does not appear to be expanding. To achieve this, the factor of a^2 is removed such that $T_{\mu\nu}$ = diag(ρ,a^2p_x,a^2p_y,a^2p_z) becomes $T^\mu{}_\nu$ = diag($-\rho$,p_x,p_y,p_z). By assuming a spatially homogeneous field φ (*i.e. its spatial derivatives are zero*), we see from Equation 4.1 that the energy density $\rho = -T^0{}_0$ and pressure $p = T^i{}_i$ for i = 1, 2, 3 of the field φ in the local rest frame of an observer are given by

$$\rho = -T^0{}_0 = -\partial^0\varphi\partial_0\varphi + g^0{}_0\left[\frac{1}{2}\partial^\alpha\partial_\alpha\varphi + V(\varphi)\right] = \dot{\varphi}^2 - \frac{1}{2}\dot{\varphi}^2 + V(\varphi),$$

$$p = T^i{}_i = \partial_i\varphi\partial_i\varphi - g^i{}_i\left[\frac{1}{2}\partial^\alpha\partial_\alpha\varphi + V(\varphi)\right] = 0 + \frac{1}{2}\dot{\varphi}^2 - V(\varphi), \tag{4.2}$$

leading to the following EoS:

$$w = \frac{p}{\rho} = \frac{\dot{\varphi}^2/2 - V(\varphi)}{\dot{\varphi}^2/2 + V(\varphi)}. \tag{4.3}$$

We see from Equation 4.3 that w can only range from −1 (when V tends to infinity, making $\dot{\varphi}^2/2$ negligible) to 1 (when $\dot{\varphi}^2/2$ tends to infinity, making V negligible). The EoS can also be written using the Chevallier-Polarski-Linear (CPL) parametrization (Chevallier & Polarski, 2001), a common parametrization found in literature which uses the cosmological scale factor a, w_0 (the present-day value of w with a = 1), and $w_a = -\mathrm{d}w/\mathrm{d}a$ evaluated at a = 1; it is a first-order Taylor

expansion around $a = 1$ and linearly approximates non-linear solutions to w for high-a (i.e. the plot of w against a using CPL is a straight line). The CPL parametrization is given by (Bayat & Hertzberg, 2025)

$$w(a) = w_0 + w_a(1 - a) . \tag{4.4}$$

From Equation 4.4, we see that $w_0 = 0$ and $w_a = 1$ for ΛCDM. We refer to the cosmological model that assumes cold dark matter (CDM) and the CPL parametrization as the w_0w_aCDM model. For quintessence, since $w \geq -1$, any region where $w < -1$ is called the phantom region (which corresponds to the phantom dark energy model). Thus, the line $w = -1$ is called the phantom divide line (PDL). To compare different dark energy models, this paper looks at the predicted evolution of w with respect to a and z and how it correlates with observational data. There are different classes of quintessence models, with the two main types being freezing ($w_a < 0$) and thawing ($w_a > 0$) models. The idea behind having differing models of quintessence is that, even though the potential field decreases towards a minimum, its rate of decrease could vary at different epochs of the universe, and this results in different behaviors of the quintessence EoS and predicted evolutions of the universe. The scalar field φ follows the same equation of motion in both types (Bayat & Hertzberg, 2025; Chevallier & Polarski, 2001; Perivolaropoulos & Skara, 2022; Spergel et al., 2007):

$$\ddot{\varphi} + 3H\dot{\varphi} + V'(\varphi) = 0 , \tag{4.5}$$

where H is Hubble's parameter and V' is the derivative of V with respect to φ. The above equation determines how the scalar field φ will evolve, given its acceleration $\ddot{\varphi}$, its effect due to Hubble friction $3H\dot{\varphi}$, and the rate of change of its potential energy V (which is what decelerates φ). The above equation can then be used to deduce the predicted evolution of w for quintessence models. An example freezing model potential is given by

$$\mathrm{V_f}(\varphi) = M^{4+\beta}\varphi^{-\beta} , \tag{4.6}$$

where M is the mass parameter (a quantity that makes the quintessence scalar field energy density match the observed value of the dark energy density ρ_Λ) constrained to be less than or approximately 1.78×10^{-39} kg (Khoury, 2013; Khoury & Weltman, 2004) and $\beta > 0$ is a constant. The idea behind freezing models is that in the early stages of the universe, $w > -1$ and $\mathrm{V_f}$ had already been decreasing towards a minimum, but as time passes, its rate of decrease slows down and tends towards $w = -1$. This is shown through the exponential term $\varphi^{-\beta}$. An example thawing model potential is given by

$$V_\mathrm{t}(\varphi) = M^4\left[1 + \cos\left(\frac{\varphi}{f}\right)\right], \tag{4.7}$$

where f is a constant representing the width of $\mathrm{V_t}$. The idea behind thawing models is that, in a sense "opposite" to freezing models, $w \approx -1$ and $\mathrm{V_t}$ remains constant in the early stages, and then w increases with time as $\mathrm{V_t}$ starts to decrease to its minimum. This occurs due to the Hubble friction term in Equation (4.5), $3H\dot{\varphi}$, which causes the initial dampening of $\mathrm{V_t}$ (causing its initial constancy) (Caldwell & Linder, 2005; Tsujikawa, 2013; Yoo & Watanabe, 2012). The EoS of the freezing potential (Equation 4.6) is given by (Chiba et al., 2013; Tsujikawa, 2013)

$$w_f(a) = w_0 + \sum_{n=1}^{\infty} \frac{(-1)^{n-1} w_0 (1 - w_0^2)}{1 - w_0(n+1) + 2n w_0^2 (n+1)} \left[\frac{\Omega_\varphi(a)}{1 - \Omega_\varphi(a)} \right]^n , \tag{4.8}$$

where $\Omega_\varphi(a) = \rho_\varphi / (3H^2 M_{pl}^2)$ is the field density parameter of φ, ρ_φ is the energy density of φ, H is the Hubble parameter, and M_{pl} is the Planck mass. The term $\Omega_\varphi(a)/[1 - \Omega_\varphi(a)]$ "tracks" how much dark energy and matter dominate throughout the universe's history and thus determines the rate of evolution of w_f. The 3rd-order analytical solution to $w_f(a)$ for the freezing potential (Equation 4.8) is plotted in Figure 2.

The EoS of the thawing potential (Equation 4.7) is given by

$$w_t(a) = -1 + (1 + w_0) a^{3(K-1)} \widetilde{F}(a) , \tag{4.9}$$

where we define the quantities K and $F(a)$ as

$$K \equiv \sqrt{1 - \frac{4M_{pl}^2 V''}{3V}}, \qquad F(a) \equiv \sqrt{1 + \left(\Omega_{\varphi 0}^{-1} - 1 \right) a^{-3}} , \tag{4.10}$$

such that $\widetilde{F}(a)$ is given more concisely by

$$\widetilde{F}(a) = \left[\frac{(K - F)(F + 1)^K + (K + F)(F - 1)^K}{\left(K - \Omega_{\varphi 0}^{-\frac{1}{2}} \right) \left(\Omega_{\varphi 0}^{-\frac{1}{2}} + 1 \right)^K + \left(K + \Omega_{\varphi 0}^{-\frac{1}{2}} \right) \left(\Omega_{\varphi 0}^{-\frac{1}{2}} - 1 \right)^K} \right]^2 , \tag{4.11}$$

where $\Omega_{\varphi 0} \approx 0.7$ is the present-day value of Ω_φ (Tsujikawa, 2013). The term $a^3(K - 1)$ controls how fast w_t grows; a larger K means a faster thawing. K describes the curvature of V (given by the second derivative of V) and thus also correlates with the rate at which wt grows. F depends on the curvature parameter of dark energy and tends towards $1/\Omega_{\varphi 0}$ as a goes to 1. $\widetilde{F}$ therefore takes into account both the shape of the potential energy of quintessence and its relative dominance compared to matter. Analytical solutions to $w_t(a)$ for the thawing potential (Equation 4.9) with $K = 1.9$, 2.9, and 8.2 are plotted in Figure 3.

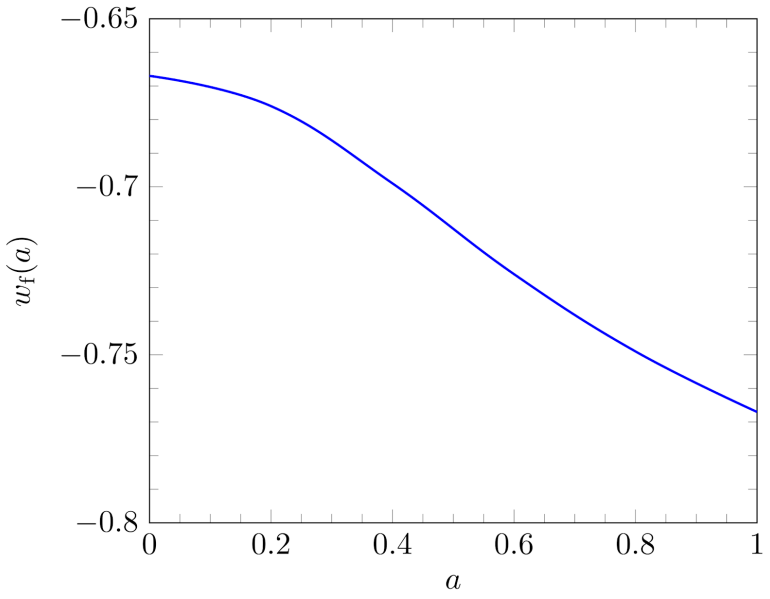

Figure 2. Plot of the 3rd-order analytical solution to $w_f(a)$ (Equation 4.8) against the scale factor a for the freezing potential (Equation 4.6) with $\beta = 1$. Reproduced from (Tsujikawa, 2013).

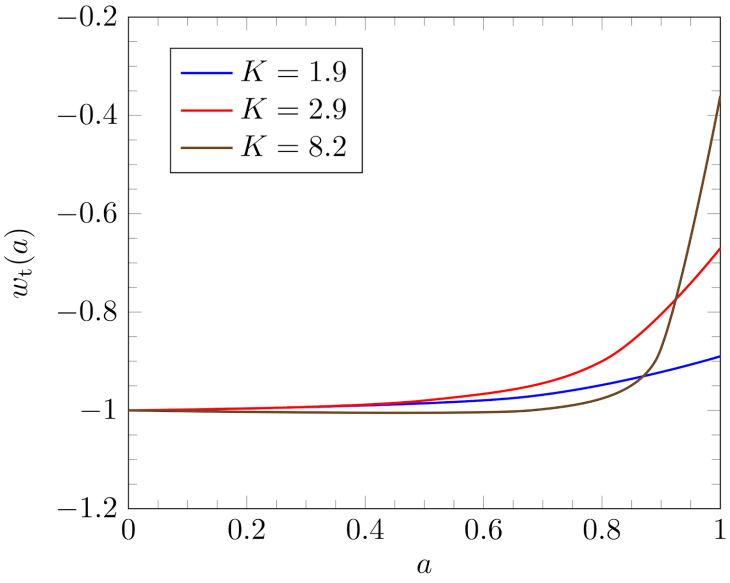

Figure 3. Plot of the analytical solution to $w_t(a)$ (Equation 4.9) against the scale factor a for the thawing potential (Equation 4.7) with K = 1.9, 2.9, and 8.2. Reproduced from (Tsujikawa, 2013).

5. Results and Discussion

The previous section reviewed freezing and thawing models of quintessence. In 2025, the Dark Energy Spectroscopic Instrument (DESI) released data from BAO measurements from more than 14 million galaxies and quasars, which were used to constrain various cosmological parameters (Abdul-Karim et al., 2025). The EoS of freezing and thawing models with CPL constraints from the DESI DR2 data are compared; these are plotted in Figure 4.

From Figure 4, we see that the ΛCDM model falls within the green bands only within around $0.6 < a < 0.75$, but does not deviate as significantly when compared to the freezing model. Thus, ΛCDM is not completely ruled out based solely on CPL constraints. We see from Figure 4a that the freezing model deviates significantly for $a < 0.8$—well beyond the 95% confidence region when compared to DESI measurements, thus not favored by observations. The thawing model in Figure 4b with $K = 2.9$ falls within the 68% and 95% confidence regions for $0.7 < a < 1$, but deviates more significantly for $a < 0.5$. However, deviations are expected since CPL is only a linear parametrization in a, and many quintessence potentials lead to a non-linear w (with examples including the freezing and thawing models in this paper; see Figures 2 and 3). This means that CPL only approximates a local region of a predicted EoS (Linden & Virey, 2008), as seen in Figure 4, with good approximation around $0.6 < w < 1$.

From Figure 4, we also see that at around $a \approx 0.7$, it is likely that w crossed the PDL, corresponding to a transition between quintessence and phantom dark energy models. Phantom dark energy is modelled with a potential φ and a negative kinetic energy component; it is characterized by $w \leq -1$. Its EoS is given by

$$w = \frac{p}{\rho} = \frac{-\dot{\phi}/2 - V(\phi)}{-\dot{\phi}/2 + V(\phi)}. \tag{5.1}$$

However, even a purely phantom dark energy model would not satisfy the green bands in Figure 4 for $a > 0.7$. An analysis conducted by Lodha et al. (2025) also showed that freezing and thawing models lack strong support from observational data. This indicates a main weakness of quintessence, which is that its predictions of the equation of state do not correlate very strongly with observational evidence and deviates for smaller values of a. Feng et al. (2005) proposed a quintom model (a portmanteau of quintessence and phantom) where w was allowed to transition between quintessence and phantom behavior.

Higher-order parametrizations based on CPL have also been proposed and analyzed to better approximate dark energy models (Nesseris et al., 2025). An extended parametrization based on CPL is given by

$$w(a) = w_0 + w_a(1 - a) + w_b(1 - a)^2, \tag{5.2}$$

where w_0 is the present-day value of w, $w_a = -\mathrm{d}w/\mathrm{d}a$ at $a = 1$, and $w_b = -(\mathrm{d}^2w/\mathrm{d}a^2)/2$ at $a = 1$. Models assuming CDM and the extended CPL parametrization given by Equation 5.2 are dubbed $w_0w_aw_b$CDM. Figure 5 compares freezing and thawing quintessence EoS with $w_0w_aw_b$CDM constraints from the 2024 DESI DR1.

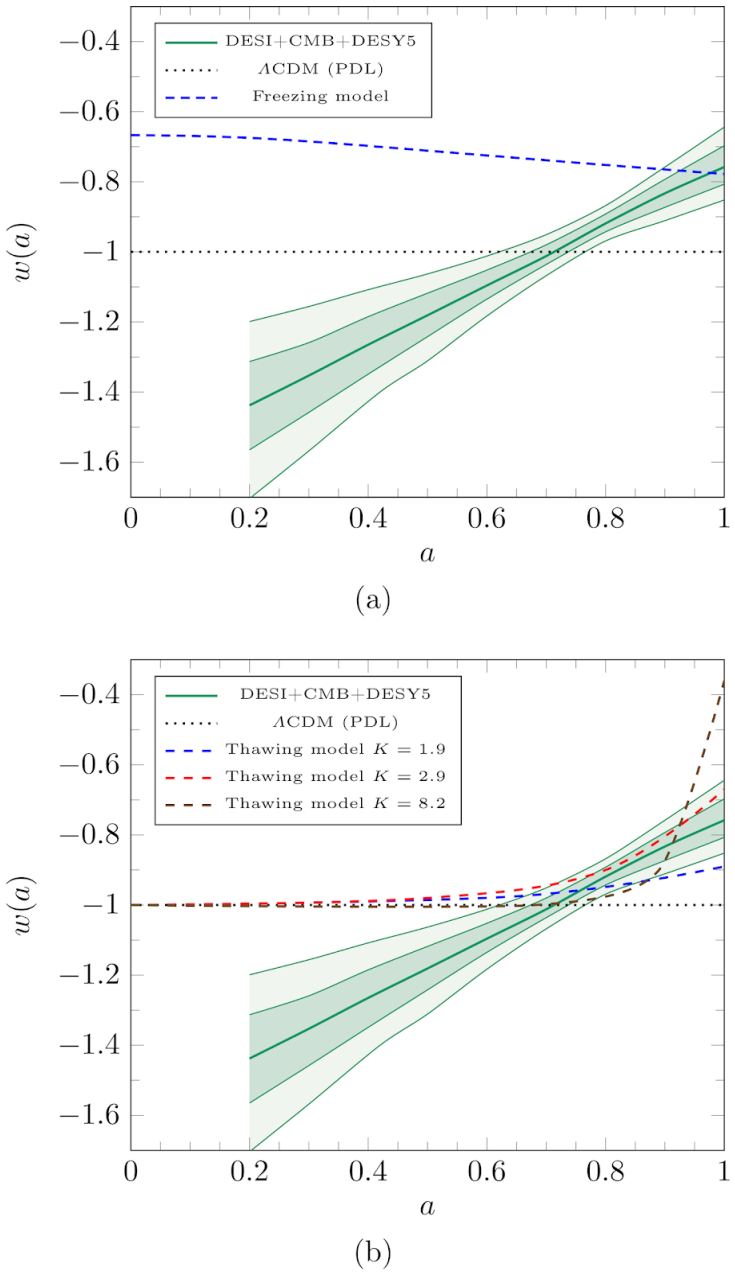

Figure 4: Plots of the EoS w(a) using CPL (green) against scale factor a for freezing (a) and thawing (b) quintessence models for K = 1.9 (blue), 2.9 (red), and 8.2 (brown) with observational constraints from the 2025 DESI DR2. The solid green curve represents the observed best fit of w for CPL, and the dark- and light-green bands around it represent a 68% and 95% confidence region for CPL, respectively. Reproduced from (Abdul-Karim et al., 2025).

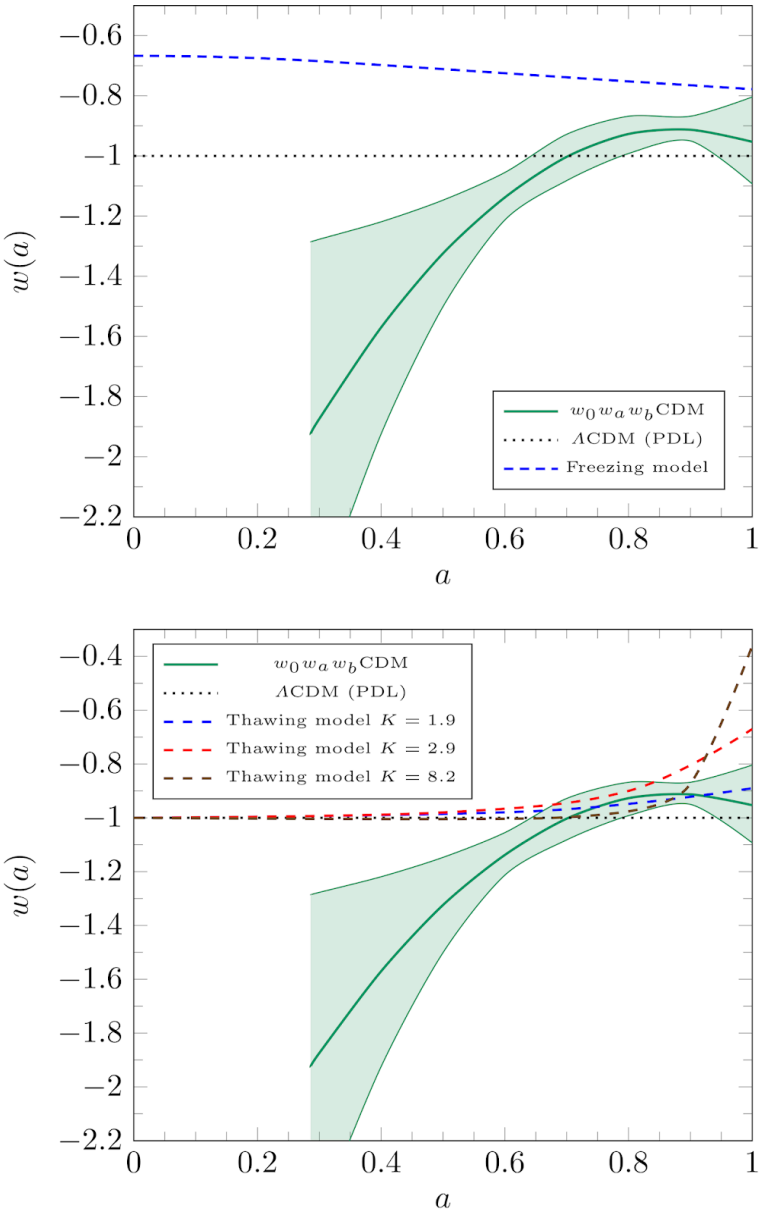

Figure 5: Plots of the EoS w(a) using extended CPL parametrization against scale factor a for freezing (top) and thawing (bottom) quintessence models with observational constraints from the 2024 DESI DR1. The solid green curve represents the observed best fit of w under extended CPL parametrization, and the green band around it represents a 68% confidence region for extended CPL. Reproduced from (Abdul-Karim et al., 2025) and (Nesseris et al., 2025).

The DESI collaboration also provided measurements of the possible ranges for w_0 and wa for the CPL parametrization of w (Abdul-Karim et al., 2025), shown in Figure 6. We see that the point with $w_0 = -1$ and $w_a = 0$, corresponding to ΛCDM, falls outside the 68% and 95% confidence regions, with the DESI data rejecting ΛCDM with confidence 2.8–4.2σ, providing relatively consistent results favoring $w_0 > 1$ and $w_a < 0$. Wolf et al. (2024) showed that there is minimal overlap between the predicted and observed regions for w0 and wa for thawing models. However, their analysis used the potential $V(\varphi) = V_0 + m^2\varphi^2/2$, which they argued represents various potentials and covers a wide range of values for w_0 and w_a. This partially agrees with results from this paper, where it is found that the thawing EoS in Equation 4.9 meaningfully overlaps for $0.7 < a < 1$.

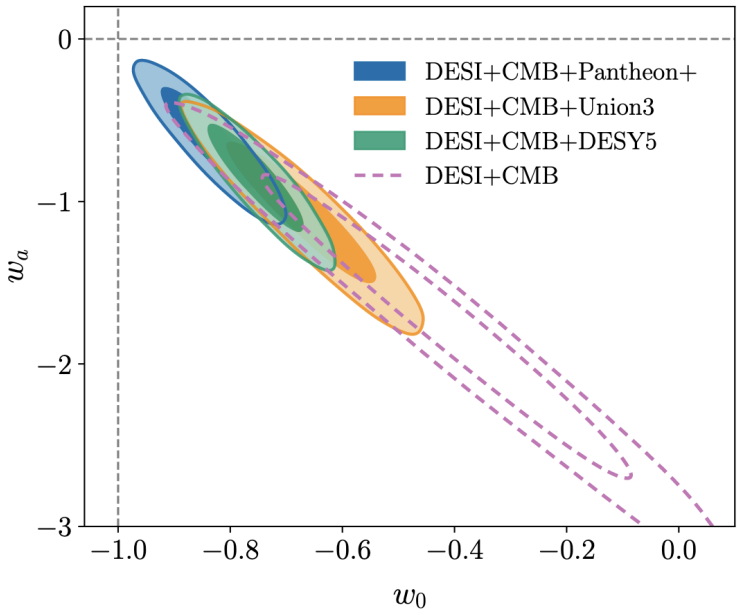

Figure 6. Contour plots of the posterior distributions of w_0 and w_a, with the darker and lighter regions (or the smaller and larger curves) representing a 68% and 95% confidence level, respectively. The intersection of the grey dashed lines represents the values of w_0 and w_a for ΛCDM. Image from (Abdul-Karim et al., 2025).

Lodha et al. (2025) conducted further analysis of the DESI DR2 data to test the consistency of dynamic dark energy models for a broad range of functional forms of w. They compared various parametrizations, including the CPL, Barboza-Alcaniz (BA), exponential (EXP), logarithmic (LOG), and Jassal-Bagla-Padmanabhan (JBP) parametrizations, also including an EoS written in terms of Chebyshev polynomials. They found that the resultant form of w is still relatively consistent with observations, having little dependence on which parametrization is used for a dynamical dark energy model. Lodha et al. also used a binning approach, an unbiased method of comparing w at different redshift intervals without assuming a functional form of w. This ensures that the evolution of the universe's expansion (e.g., through w and the FEs) can be reconstructed with minimal presumptions about the specific model of dark energy. Figures 7 and 8 compare the data from binning and constraints for w_0w_aCDM and $w_0w_aw_b$CDM, respectively.

These results suggest evidence for a quintom scenario (i.e., w_0w_aCDM, $w_0w_aw_b$CDM, and the like), with $w_0w_aw_b$CDM appearing to fit the binning data slightly better than w_0w_aCDM (although with more uncertainty at low-a regions). Despite this, alternative parametrizations or models are still not ruled out — including ΛCDM — since current observations are unable to measure w precisely for non-local (smaller) values of a. CPL and extended CPL are also only Taylor approximations about $a = 1$, so higher-order behavior in a of w potentially cannot be captured by these parametrizations.

In the analysis of the DESI data by Gialamas et al. (2025), however, it is argued that although phantom behavior is suggested by observational data, it is not statistically robust as pure quintessence behavior with $w \geq -1$ is still supported with 2σ confidence. In their analysis, they included a Higgs-like quintessence (HLQ) model without phantom behavior; despite CPL matching observational data slightly better than HLQ, HLQ is motivated through physical theory, unlike CPL, which was developed only to parametrize and fit observational data (Gialamas et al., 2025).

The reason for varied predicted evolutions of w from different dark energy parametrizations and models is due to degeneracy, which is the idea that many different models of dark energy can give rise to the same cosmological observations, and our current observational data is not sensitive enough to distinguish the different scenarios for w at high-z (low-a) (Marttens et al., 2020).

From all the above figures and available data, this paper concludes that the current data favors dynamical dark energy over ΛCDM with fairly high confidence, although current instruments are not sensitive enough to differentiate between particular dark energy models, so multiple dark energy models leading to similar EoS or predicted evolutions of the universe cannot be ruled out. The EoS from ΛCDM also does not deviate significantly enough from observational data for this paper to conclude with high confidence that ΛCDM is implausible. Moreover, using data from the unbiased binning method for measuring the dark energy EoS, this paper concludes that there is some indication of the EoS involving phantom behavior (i.e. that it crosses the PDL).

Even if we do manage to further constrain the EoS, issues like the Hubble tension would still prevent a conclusive decision on a correct dark energy model. The conflict between QFT, general relativity, and observational measurements of the vacuum energy density further implies a fundamental flaw in our mathematical descriptions of dark energy. Quintessence also does not solve the coincidence problem fully as it still requires fine-tuning, essentially moving the question from “why this specific value?” to “why this potential?”, and thus more physically motivated models like chameleon particles or modified gravity models are more likely alternatives. A development in the theory behind dark energy that explains the initial potential value would strengthen the plausibility of quintessence.

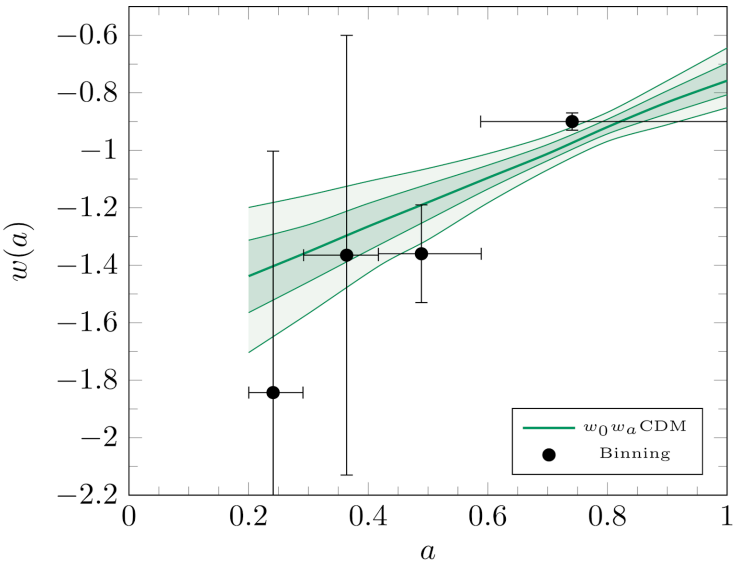

Figure 7: A comparison between w_0w_aCDM constraints (with the dark- and light-green contours representing 68% and 95% confidence regions) and data from the binning method. The black bins represent a 1σ error. Reproduced from (Abdul-Karim et al., 2025).

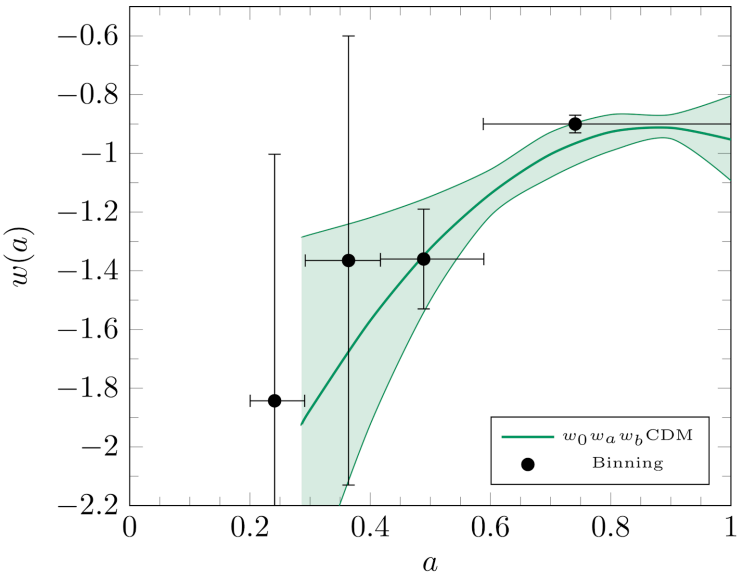

Figure 8: A comparison between $w_0w_aw_b$CDM constraints (with the dark-green contours representing a 68% confidence region) and data from the binning method. The black bins represent a 1σ error. Reproduced from (Abdul-Karim et al., 2025) and (Nesseris et al., 2025).

6. Conclusion

In this paper, the main pieces of evidence supporting the accelerated expansion of the universe were discussed, and the development of alternative dark energy theories is motivated by discussing current issues with ΛCDM. Then, the core concepts of ΛCDM were reviewed, and the basic physics of quintessence were explored. The predicted EoS from quintessence to observational data from the DESI collaboration was compared, and it was found that quintessence is a more preferred model than ΛCDM. However, due to strong evidence for a phantom crossing, it is concluded that neither quintessence nor phantom fully matches observational data. It is instead found that models including w_0w_aCDM and $w_0w_aw_b$CDM fit observational data better, with dynamical dark energy models being more favorable than constant ones.

However, this paper is not a comprehensive review of all dark energy models; only particular modified matter models (with an emphasis on quintessence) and how closely their predictions fit observational data were focused on. Hence, further comparisons and research into other modified matter models (such as K-essence, Chaplygin gas, and chameleon) and modified gravity models (such as $f(R)$ gravity, modified Newtonian dynamics, and DGP braneworld) (Yoo & Watanabe, 2012) are needed. Furthermore, because current observations do not allow high distinguishability between certain dark energy models and parametrization, this paper concludes that ΛCDM is still a feasible model, but is seemingly slowly being ruled out. Further development in observational techniques is required.

This paper also mainly focused on comparing predicted evolutions of the EoS for each model; there are, however, other methods of assessing the plausibility of a model, such as its mathematical complexity and the number of parameters required to describe the model. Further analysis of dark energy models, especially of phantom and quintom, is deferred to future work.

7. References

Abbott, T., Abdalla, F. B., Aleksić, J., Allam, S., Amara, A., Bacon, D., Balbinot, E., Banerji, M., Bechtol, K., Benoit-Lévy, A., Bernstein, G. M., Bertin, E., Blazek, J., Bonnett, C., Bridle, S., Brooks, D., Brunner, R. J., Buckley-Geer, E., Burke, D. L., … Zuntz, J. (2016). The Dark Energy Survey: More than dark energy – an overview. *Monthly Notices of the Royal Astronomical Society*, 460(2), 1270–1299. https://doi.org/10.1093/mnras/stw641

Abbott, T. M. C., Acevedo, M., Aguena, M., Alarcon, A., Allam, S., Alves, O., Amon, A., Andrade-Oliveira, F., Annis, J., Armstrong, P., Asorey, J., Avila, S., Bacon, D., Bassett, B. A., Bechtol, K., Bernardinelli, P. H., Bernstein, G. M., Bertin, E., Blazek, J., … Zhang, Y. (2025). *The Dark Energy Survey: Cosmology results with ~1500 new high-redshift type Ia supernovae using the full 5-year dataset* (arXiv:2401.02929). arXiv. https://doi.org/10.48550/arXiv.2401.02929

Abbott, T. M. C., Adamow, M., Aguena, M., Allam, S., Alves, O., Amon, A., Andrade-Oliveira, F., Asorey, J., Avila, S., Bacon, D., Bechtol, K., Bernstein, G. M., Bertin, E., Blazek, J., Bocquet, S., Brooks, D., Burke, D. L., Camacho, H., Rosell, A. C., … Yanny, B. (2024). *Dark Energy Survey: A 2.1% measurement of the angular baryonic acoustic oscillation scale at redshift z_eff = 0.85 from the final dataset* (arXiv:2402.10696). arXiv. https://doi.org/10.48550/arXiv.2402.10696

Abdul-Karim, M., Aguilar, J., Ahlen, S., Alam, S., Allen, L., Prieto, C. A., Alves, O., Anand, A., Andrade, U., Armengaud, E., Aviles, A., Bailey, S., Baltay, C., Bansal, P., Bault, A., Behera, J., BenZvi, S., Bianchi, D., Blake, C., … Zou, H. (2025). *DESI DR2 results II:*

Measurements of baryon acoustic oscillations and cosmological constraints (arXiv:2503.14738). arXiv. https://doi.org/10.48550/arXiv.2503.14738

Aghanim, N., Akrami, Y., Ashdown, M., Aumont, J., Baccigalupi, C., Ballardini, M., Banday, A. J., Barreiro, R. B., Bartolo, N., Basak, S., Battye, R., Benabed, K., Bernard, J.-P., Bersanelli, M., Bielewicz, P., Bock, J. J., Bond, J. R., Borrill, J., Bouchet, F. R., … Zonca, A. (2020). Planck 2018 results. VI. Cosmological parameters. *Astronomy & Astrophysics*, 641, Article A6. https://doi.org/10.1051/0004-6361/201833910

Bamonti, N., & Thébault, K. P. Y. (2025). *In search of cosmic time: Complete observables and the clock hypothesis* (arXiv:2411.00541). arXiv. https://doi.org/10.48550/arXiv.2411.00541

Bayat, Z., & Hertzberg, M. P. (2025). *Examining quintessence models with DESI data* (arXiv:2505.18937). arXiv. https://doi.org/10.48550/arXiv.2505.18937

Blake, C., Davis, T., Poole, G., Parkinson, D., Brough, S., Colless, M., Contreras, C., Couch, W., Croom, S., Drinkwater, M. J., Forster, K., Gilbank, D., Gladders, M., Glazebrook, K., Jelliffe, B., Jurek, R. J., Li, I.-H., Madore, B., Martin, C., … Yee, H. (2011). The WiggleZ Dark Energy Survey: Testing the cosmological model with baryon acoustic oscillations at z = 0.6. *Monthly Notices of the Royal Astronomical Society*, 415(3), 2892–2909. https://doi.org/10.1111/j.1365-2966.2011.19077.x

Caldwell, R. R., Dave, R., & Steinhardt, P. J. (1998). Cosmological imprint of an energy component with general equation of state. *Physical Review Letters*, 80(8), 1582–1585. https://doi.org/10.1103/PhysRevLett.80.1582

Caldwell, R. R., & Linder, E. V. (2005). The limits of quintessence. *Physical Review Letters*, 95(14), Article 141301. https://doi.org/10.1103/PhysRevLett.95.141301

Chandrasekhar, S. (1931). The maximum mass of ideal white dwarfs. *The Astrophysical Journal*, 74, 81–82. https://doi.org/10.1086/143324

Chevallier, M., & Polarski, D. (2001). Accelerating universes with scaling dark matter. *International Journal of Modern Physics D*, 10(2), 213–223. https://doi.org/10.1142/S0218271801000822

Chiba, T., De Felice, A., & Tsujikawa, S. (2013). Observational constraints on quintessence: Thawing, tracker, and scaling models. *Physical Review D*, 87(8), Article 083505. https://doi.org/10.1103/PhysRevD.87.083505

Coble, K., Nickerson, M. D., Bailey, J. M., Trouille, L. E., Cochran, G. L., Camarillo, C. T., & Cominsky, L. R. (2013). Investigating student ideas about cosmology II: Composition of the universe. *Astronomy Education Review*, 12(1), Article 010108. https://doi.org/10.3847/aer2012039

Copeland, E. J., Sami, M., & Tsujikawa, S. (2006). Dynamics of dark energy. *International Journal of Modern Physics D*, 15(11), 1753–1935. https://doi.org/10.1142/S021827180600942X

Einstein, A. (1915). Die Feldgleichungen der Gravitation [The field equations of gravitation]. *Sitzungsberichte der Preussischen Akademie der Wissenschaften zu Berlin*, 844–847. https://doi.org/10.1002/3527608958.ch5

Einstein, A. (1917). *Kosmologische Betrachtungen zur allgemeinen Relativitätstheorie* [Cosmological considerations in the general theory of relativity]. https://ia601503.us.archive.org/13/items/einstein-kosmologische-betrachtungen-zur-allgemeinen-relativitatstheorie/%281917%29%20Einstein%20A.%20-%20Kosmologische%20Betrachtungen%20zur%20allgemeinen%20Relativitätstheorie.pdf

Eisenstein, D. J., Zehavi, I., Hogg, D. W., Scoccimarro, R., Blanton, M. R., Nichol, R. C., Scranton, R., Seo, H., Tegmark, M., Zheng, Z., Anderson, S., Annis, J., Bahcall, N., Brinkmann, J., Burles, S., Castander, F. J., Connolly, A., Csabai, I., Doi, M., … York, D. (2005). Detection of the baryon acoustic peak in the large-scale correlation function of SDSS luminous red galaxies. *The Astrophysical Journal*, 633(2), 560–574. https://doi.org/10.1086/466512

Feng, B., Wang, X., & Zhang, X. (2005). Dark energy constraints from the cosmic age and supernova. *Physics Letters B*, 607(1–2), 35–41. https://doi.org/10.1016/j.physletb.2004.12.071

Friedmann, A. (1922). Über die Krümmung des Raumes [On the curvature of space]. *Zeitschrift für Physik*, 10, 377–386. https://doi.org/10.1007/BF01332580

Gialamas, I. D., Hütsi, G., Raidal, M., Urrutia, J., Vasar, M., & Veermäe, H. (2025). Quintessence and phantoms in light of DESI 2025 (arXiv:2506.21542). arXiv. https://doi.org/10.48550/arXiv.2506.21542

Gu, J.-A., Chen, C.-W., & Chen, P. (2009). A new approach to testing dark energy models by observations. *New Journal of Physics*, 11(7), Article 073029. https://doi.org/10.1088/1367-2630/11/7/073029

Hubble, E. (1929). A relation between distance and radial velocity among extra-galactic nebulae. *Proceedings of the National Academy of Sciences*, 15(3), 168–173. https://doi.org/10.1073/pnas.15.3.168

Janka, H.-T., Langanke, K., Marek, A., Martinez-Pinedo, G., & Mueller, B. (2007). Theory of core-collapse supernovae. *Physics Reports*, 442(1–6), 38–74. https://doi.org/10.1016/j.physrep.2007.02.002

Khoury, J. (2013). Chameleon field theories. *Classical and Quantum Gravity*, 30(21), Article 214004. https://doi.org/10.1088/0264-9381/30/21/214004

Khoury, J., & Weltman, A. (2004). Chameleon cosmology. *Physical Review D*, 69(4), Article 044026. https://doi.org/10.1103/PhysRevD.69.044026

Li, M., Li, X.-D., Wang, S., & Wang, Y. (2011). Dark energy. *Communications in Theoretical Physics*, 56(3), 525–604. https://doi.org/10.1088/0253-6102/56/3/24

Liddle, A. R., Mukherjee, P., Parkinson, D., & Wang, Y. (2006). Present and future evidence for evolving dark energy. *Physical Review D*, 74(12), Article 123506. https://doi.org/10.1103/PhysRevD.74.123506

Linden, S., & Virey, J.-M. (2008). A test of the CPL parameterization for rapid dark energy equation of state transitions. *Physical Review D*, 78(2), Article 023526. https://doi.org/10.1103/PhysRevD.78.023526

Lodha, K., Calderon, R., Matthewson, W. L., Shafieloo, A., Ishak, M., Pan, J., Garcia-Quintero, C., Huterer, D., Valogiannis, G.,

Ureña-López, L. A., Kamble, N. V., Parkinson, D., Kim, A. G., Zhao, G. B., Cervantes-Cota, J. L., Rohlf, J., Lozano-Rodríguez, F., Román-Herrera, J. O., Abdul-Karim, M., … Zou, H. (2025). *Extended dark energy analysis using DESI DR2 BAO measurements* (arXiv:2503.14743). arXiv. https://doi.org/10.48550/arXiv.2503.14743

Marttens, R. von, Lombriser, L., Kunz, M., Marra, V., Casarini, L., & Alcaniz, J. (2020). Dark degeneracy I: Dynamical or interacting dark energy? *Physics of the Dark Universe*, 28, Article 100490. https://doi.org/10.1016/j.dark.2020.100490

Mayet, F., Green, A. M., Battat, J. B. R., Billard, J., Bozorgnia, N., Gelmini, G. B., Gondolo, P., Kavanagh, B. J., Lee, S. K., Loomba, D., Monroe, J., Morgan, B., O'Hare, C. A. J., Peter, A. H. G., Phan, N. S., & Vahsen, S. E. (2016). A review of the discovery reach of directional dark matter detection. *Physics Reports*, 627, 1–49. https://doi.org/10.1016/j.physrep.2016.02.007

Nesseris, S., Akrami, Y., & Starkman, G. D. (2025). *To CPL, or not to CPL? What we have not learned about the dark energy equation of state* (arXiv:2503.22529). arXiv. https://doi.org/10.48550/arXiv.2503.22529

Peebles, P. J. E., & Ratra, B. (2003). The cosmological constant and dark energy. *Reviews of Modern Physics*, 75(2), 559–606. https://doi.org/10.1103/RevModPhys.75.559

Perivolaropoulos, L., & Skara, F. (2022). Challenges for ΛCDM: An update. *New Astronomy Reviews*, 95, Article 101659. https://doi.org/10.1016/j.newar.2022.101659

Perlmutter, S., Aldering, G., Goldhaber, G., Knop, R. A., Nugent, P., Castro, P. G., Deustua, S., Fabbro, S., Goobar, A., Groom, D. E., Hook, I. M., Kim, A. G., Kim, M. Y., Lee, J. C., Nunes, N. J., Pain, R., Pennypacker, C. R., Quimby, R., Lidman, C., … Couch, W. J. (1999). Measurements of Omega and Lambda from 42 high-redshift supernovae. *The Astrophysical Journal*, 517(2), 565–586. https://doi.org/10.1086/307221

Riess, A. G., Casertano, S., Yuan, W., Macri, L. M., & Scolnic, D. (2019). Large Magellanic Cloud Cepheid standards provide a 1% foundation for the determination of the Hubble constant and stronger evidence for physics beyond LambdaCDM. *The Astrophysical Journal*, 876(1), Article 85. https://doi.org/10.3847/1538-4357/ab1422

Riess, A. G., Filippenko, A. V., Challis, P., Clocchiattia, A., Diercks, A., Garnavich, P. M., Gilliland, R. L., Hogan, C. J., Jha, S., Kirshner, R. P., Leibundgut, B., Phillips, M. M., Reiss, D., Schmidt, B. P., Schommer, R. A., Smith, R. C., Spyromilio, J., Stubbs, C., Suntzeff, N. B., & Tonry, J. (1998). Observational evidence from supernovae for an accelerating universe and a cosmological constant. *The Astronomical Journal*, 116(3), 1009–1038. https://doi.org/10.1086/300499

Sandage, A. (1962). The change of redshift and apparent luminosity of galaxies due to the deceleration of selected expanding universes. *The Astrophysical Journal*, 136, 319–333. https://doi.org/10.1086/147385

Souza, R. de, Rodrigues, G., & Alcaniz, J. (2025). *Thawing quintessence and transient cosmic acceleration in light of DESI* (arXiv:2504.16337). arXiv. https://doi.org/10.48550/arXiv.2504.16337

Spergel, D. N., Bean, R., Doré, O., Nolta, M. R., Bennett, C. L., Dunkley, J., Hinshaw, G., Jarosik, N., Komatsu, E., Page, L., Peiris, H. V., Verde, L., Halpern, M., Hill, R. S., Kogut, A., Limon, M., Meyer, S. S., Odegard, N., Tucker, G. S., … Wright, E. L. (2007). Wilkinson Microwave Anisotropy Probe (WMAP) three year results: Implications for cosmology. *The Astrophysical Journal Supplement Series*, 170(2), 377–408. https://doi.org/10.1086/513700

Steinhardt, P. J. (2003). A quintessential introduction to dark energy. Philosophical Transactions of the Royal Society of London. *Series A: Mathematical, Physical and Engineering Sciences*, 361(1812), 2497–2513. https://doi.org/10.1098/rsta.2003.1290

Tsujikawa, S. (2013). Quintessence: A review. *Classical and Quantum Gravity*, 30(21), Article 214003. https://doi.org/10.1088/0264-9381/30/21/214003

Tutusaus, I., Bonvin, C., & Grimm, N. (2024). Measurement of the Weyl potential evolution from the first three years of Dark Energy Survey data. *Nature Communications*, 15(1), Article 9295. https://doi.org/10.1038/s41467-024-53363-6

Weinberg, S. (1989). The cosmological constant problem. *Reviews of Modern Physics*, 61(1), 1–23. https://doi.org/10.1103/RevModPhys.61.1

Wolf, W. J., García-García, C., Bartlett, D. J., & Ferreira, P. G. (2024). Scant evidence for thawing quintessence. *Physical Review D*, 110(8), Article 083528. https://doi.org/10.1103/PhysRevD.110.083528

Yoo, J., & Watanabe, Y. (2012). Theoretical models of dark energy. *International Journal of Modern Physics D*, 21(12), Article 1230002. https://doi.org/10.1142/S0218271812300029

Zel'dovich, Y. B. (1968). The cosmological constant and the theory of elementary particles. *Soviet Physics Uspekhi*, 11(3), 381–393. https://doi.org/10.1070/PU1968v011n03ABEH003927

Zhou, Z., Miao, Z., Bi, S., Ai, C., & Zhang, H. (2025). *What prevents resolving the Hubble tension through late-time expansion modifications?* (arXiv:2506.23556). arXiv. https://doi.org/10.48550/arXiv.2506.23556

Zlatev, I., Wang, L., & Steinhardt, P. J. (1999). Quintessence, cosmic coincidence, and the cosmological constant. *Physical Review Letters*, 82(5), 896–899. https://doi.org/10.1103/PhysRevLett.82.896

Acknowledgements

I am sincerely grateful to my mentor, Dr. Chima McGruder, and teaching assistant, Catherine Petretti, for delivering sessions on basic astrophysics knowledge, guiding me through the research process, and reviewing drafts of my paper. I am also grateful to my peers who took the IRIS Indigo Program for providing valuable feedback on my paper.

This research paper contains data from the DESI collaboration. Any opinions and conclusions written in this paper belong to the author and do not necessarily reflect the views of the U.S. National Science Foundation, the U.S. Department of Energy, or any other related funding agencies.

Author Biography

Thatcher Lai is a year 12 student studying at Rugby School, England. He is currently studying Mathematics, Further Mathematics, Physics, and Music A-levels, with a particular interest in theoretical physics. He founded the Feynman Society at Rugby School, a physics society where students present and learn about advanced physics topics, such as quantum

mechanics, relativity, and Fourier analysis. As an avid music enjoyer, he listens to, plays, and composes jazz, classical, pop, electronic, and microtonal music, releasing some of his compositions on Tencent platforms and YouTube Music.

Mentor Contribution Statements

Dr. Chima McGruder was the author's instructor for the 6-week Indigo Research Intensive Seasonal (IRIS) course this summer. As part of the course, he gave lectures on how to do an astrophysics research project from start to finish. This included material on the basics of astrophysics, followed by the fundamentals of collecting, annotating, and understanding a specific astrophysics topic with peer-reviewed sources. Then, as the students progressed in their specific project, Dr. McGruder met with them individually to advise them on ways to improve their paper topic, structure, and content. In total, this was only a few hours of individual time with him. There were more hours spent with the TA (Catherine Petretti, see her contribution statement). Finally, at the end, he provided a detailed critique, with comments and suggestions for improvement, of their final papers. Beyond this relatively hands-off advising, the author"s paper is a product of his own independent studies and intellect. Dr. McGruder supports the publication of this paper as independent and unique scholarly work.

Catherine Petretti was the teaching assistant for the IRIS summer Astrophysics course, during which the author completed the research presented in his paper "A Fifth Fundamental Force? A Comparative Review Between ΛCDM and Quintessence." The author is an exceptionally bright student, and to the best of her knowledge, all the work that he presented in his paper is his own.

During the course, her interactions with the author were mostly over email or during individual meetings, during which he would ask questions about his research and the direction in which he should take his paper. These questions did not involve technical details of his work, but mainly focused on the scope, topic, and content of the paper in a broader sense. Her main contribution to his work was as an editor, reading through and editing his paper in detail 2-3 times before his submission. However, she has not contributed any results or analysis of my own to his work. In working with the author, she has seen that he is a very independent and dedicated student, and she hopes that this letter helps to clarify his work for the *Convergence Journal*.

AI Use Statement

The author used ChatGPT as a supplementary educational tool during the early stages of the project to clarify foundational astrophysical, mathematical, and statistical concepts (e.g., dark energy models, equations of state, posterior distributions, and plot interpretation). All such clarifications were independently verified using peer-reviewed literature and reputable online sources. ChatGPT was also consulted for high-level suggestions regarding possible models and analytical approaches, alongside guidance from the author's mentor and teaching assistant. While numerical simulations were initially considered, the final analysis relied exclusively on publicly available data. AI tools were not used to generate scientific content, paraphrase from sources, or create figures; all TikZ figures were produced independently, and all sources were properly cited. After completion of the full draft, Grammarly and ChatGPT were used only for proofreading and minor stylistic refinement.

Appendix

This paper uses special notations for derivatives. An overhead dot $\dot{} = \partial/\partial t$ denotes a derivative with respect to cosmic time t and an apostrophe $' = \mathrm{d}/\mathrm{d}\varphi$ denotes a derivative with respect to the scalar field φ.

Einstein's summation notation (ESN) is a convenient way of denoting sums of indexed terms. Consider a vector $\boldsymbol{v}$, which can be expressed as a linear combination of n basis vectors $\boldsymbol{e}_i$ with n corresponding vector components v^i (where i is the index denoting the i-th object). Upper and lower indices denote contravariance and covariance with respect to basis vectors, respectively, so a covector $\boldsymbol{\alpha} = \alpha_i \boldsymbol{\varepsilon}^i$ has covariant components α_i and contravariant basis covectors $\boldsymbol{\varepsilon}^i$. ESN simplifies the notation in such a way that the usual "capital sigma" symbol in front of a sum is omitted:

$$\boldsymbol{v} = \sum_{i=1}^{n} v^i \boldsymbol{e}_i = v^i \boldsymbol{e}_i. \tag{A.1}$$

An index of 0 represents a time component and an index of 1, 2, or 3 represents a spatial component (usually in the x, y, or z direction, respectively).